Math. Struct. in Comp. Science (2014), vol. 24, iss. 5, e240516, 14 pages.
doi:10.1017/S096012951300073X

Optimal fuzzy PID controller design for an active magnetic bearing system based on adaptive genetic algorithms†

HUNG-CHENG CHEN

Department of Electrical Engineering,
National Chin-Yi University of Technology,
Taichung, Taiwan
Email: hcchen@ncut.edu.tw

Received 20 July 2011; revised 18 August 2013

We propose an adaptive genetic algorithm (AGA) for the multi-objective optimisation design of a fuzzy PID controller and apply it to the control of an active magnetic bearing (AMB) system. Unlike PID controllers with fixed gains, a fuzzy PID controller is expressed in terms of fuzzy rules whose consequences employ analytical PID expressions. The PID gains are adaptive and the fuzzy PID controller has more flexibility and capability than conventional ones. Moreover, it can be easily used to develop a precise and fast control algorithm in an optimal design. An adaptive genetic algorithm is proposed to design the fuzzy PID controller. The centres of the triangular membership functions and the PID gains for all fuzzy control rules are selected as parameters to be determined. We also present a dynamic model of an AMB system for axial motion. The simulation results of this AMB system show that a fuzzy PID controller designed using the proposed AGA has good performance.

1. Introduction

Active magnetic bearing (AMB) systems with controlled permanent magnet electromagnets have been described elsewhere. They support a rotating body without direct contact and, because of this significant feature, are widely used for various purposes. They offer a number of practical advantages over conventional bearings, such as higher speeds, lower rotating losses, elimination of the lubrication system and lubricant contamination of the process, operation at temperature extremes and in vacuum, and longer life (Knospe 2007; Fan *et al.* 2008; Chen 2011). However, AMB applications often require the solution of very interesting and formidable control problems because of their inherent instability and the non-linear relationship between the lift force and the air gap distance (Khoo *et al.* 2010; Polajzer *et al.* 1968). The controller is a key component of AMB systems, and its performance has a direct effect on whether a magnetic bearing can work stably and without failing.

† This research was supported in part by the National Science Council of the Republic of China, under Grant Number NSC99-2622-E-167-023-CC3.

In recent decades, conventional PID controllers have been widely applied in industrial process control. This is mainly because PID controllers have simple control structures and are easy to maintain (Bennett 1987; Chen 1996). To design such a controller, the proportional, integral and derivative gains must be determined. However, a conventional PID controller may have poor control performance for non-linear and/or complex systems that have no precise mathematical models. Various types of modified traditional PID controller, such as auto-tuning and adaptive PID controllers, have been developed to overcome these difficulties (Na 2001; Lin *et al.* 2003). Since the PID gains are fixed, the main disadvantage is that they are usually lacking in flexibility and capability.

Recently, many researchers have attempted to combine conventional PID controllers with fuzzy logic (Harinath and Mann 2008; Mohan and Sinha 2008). Despite the significant improvement provided by these fuzzy PID controllers compared with their conventional counterparts, they are still subject to some disadvantages. For example, the locations of the peak of the membership functions are fixed and cannot be adjusted, and the fuzzy control rules have to be designed by hand. To overcome these weaknesses, we propose a multi-objective optimisation method for the parameter tuning of fuzzy PID controllers based on an improved adaptive genetic algorithm (AGA) to solve the control problem of an AMB system. With the proposed AGA-tuning method, a fitness function is systematically defined such that the centres of the triangular membership functions and the PID gains for all fuzzy control rules can be selected as parameters to be determined. By using adaptive crossover and mutation operators, the global search ability and convergence speed of the genetic algorithm can be significantly improved (Chambers 2001; Michalewicz 1996; Srinivas and Patnaik 1994). By incorporating both the transient performance index of the dynamic response and the control input into the fitness function and properly weighting these terms, the overall performance of the fuzzy PID controller can be optimised to give greater flexibility and capability. The performance of the resulting controller was verified through simulation.

2. Fuzzy PID controllers

Fuzzy controllers are, in essence, a kind of non-linear PID controller that take advantage of the properties of both fuzzy controllers and PID controllers by converting the experience of tuning the PID parameters into fuzzy reasoning rules. In fuzzy PID controllers, the input variables of the fuzzy rules are the error signals and their derivatives, while the output variables are the PID gains. The rules of a double input single output (DISO) fuzzy PID controller are usually expressed in the following form:

R_{ij} : IF x is A_i and y *is* B_j THEN

$$u^{ij}(t) = K_p^{ij} e(t) + K_I^{ij} \int e(t)dt + +K_D^{ij} \int \dot{e}(t)dt \tag{1}$$

where:

— x denotes $e(t)$ and $x \in X$;
— y denotes $e(t)$ and $y \in Y$, $i = 1, 2, \ldots, n$;

https://doi.org/10.1017/S096012951300073X Published online by Cambridge University Press

— $j = 1, 2, \ldots, m$;
— $u(t)$ denotes the output variable.

Using a singleton fuzzifier, sum-product inference and a centre-average defuzzifier, the output of a fuzzy PID controller is

$$u_t = \frac{\sum_{i=1}^{n} \sum_{j=1}^{m} w_{ij}(x, y) u^{ij}}{\sum_{i=1}^{n} \sum_{j=1}^{m} w_{ij}(x, y)} \tag{2}$$

where

$$w_{ij}(x, y) = A_i(x) B_j(y)$$

is the firing strength of the rule denoted by R_{ij}.

For calculational convenience, triangular functions are commonly adopted as the membership functions of the input variables. In the current paper, we assume that X and Y are the universes of discourse for input variables e and $\dot{e}$, respectively. We assume

$$\{A_i(x) \in F(X),\ i = 1, 2, \ldots, n\}$$

is a cluster of fuzzy sets on X with triangular membership functions as shown in Figure 1. The apexes of $\{A_i\}$ are denoted by x_i and satisfy $x_1 < x_2 < \ldots < x_n$. The membership functions for $\{A_i\}$ can be calculated from

$$A_i(x) = \begin{cases} (x - x_{i-1})/(x_i - x_{i-1}) & x \in [x_{i-1}, x_i],\ i = 2, 3, \ldots, n \\ (x_{i+1} - x)/(x_{i+1} - x_i) & x \in [x_{i-1}, x_i],\ i = 2, 3, \ldots, n-1 \\ 1 & x < x_1 \ or \ x > x_n. \end{cases} \tag{3}$$

As with $\{A_i\}$, we assume $\{B_j(y) \in F(Y), j1, 2, \ldots, m\}$ is also a cluster of fuzzy sets on Y with the triangular membership functions given in Figure 1, the apexes of $\{B_j\}$ are denoted by y_j and satisfy

$$y_1 < y_2 < \ldots < y_m.$$

The membership functions for $\{B_j\}$ can be calculated by

$$B_j(y) = \begin{cases} (y - y_{j-1})/(y_i - y_{i-1}) & y \in [y_{i-1}, y_i],\ j = 2, 3, \ldots, m \\ (y_{i+1} - y)/(y_{i+1} - y_i) & y \in [y_{i-1}, y_i],\ j = 1, 2, 3, \ldots, m-1 \\ 1 & y < y_1 \ or \ y > y_m. \end{cases} \tag{4}$$

The base plane of the rule can be decomposed into many inference cells (ICs) with output rules on its four corners, as shown in Figure 1. The inference can then be operated on these ICs. If we assume that x_i and x_{i+1} are any two adjacent apexes of $\{A_i\}$, and y_j, and y_{j+1} are any two adjacent apexes of $\{B_j\}$, then

$$x_i \leqslant x \leqslant x_{i+1}$$
$$y_j \leqslant y \leqslant y_{j+1}$$

forms an inference cell $IC(i, j)$ in the $X \times Y$ input space – see Figure 1. For the activated inference cell $IC(i, j)$, the output of the fuzzy PID controller adopts dualistic piecewise interpolation functions of the parameters of the rule consequences, as follows (Xiu and

https://doi.org/10.1017/S096012951300073X Published online by Cambridge University Press

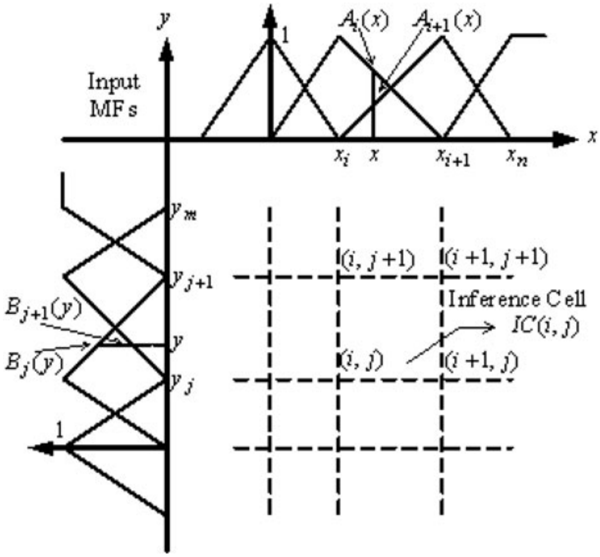

Fig. 1. The membership function for (A_i) and (B_j)

Ren 2004):

$$
\begin{aligned}
u(t) = &\left[\sum_{s=i}^{i+1}\sum_{t=j}^{j+1} w_{st}(x,y)K_p^{st}\right] e(t) + \left[\sum_{s=i}^{i+1}\sum_{t=j}^{j+1} w_{st}(x,y)K_I^{st}\right]\int e(t)dt \\
&+ \left[\sum_{s=i}^{i+1}\sum_{t=j}^{j+1} w_{st}(x,y)K_D^{st}\right]\psi(t)
\end{aligned}
\tag{5}
$$

Equation (5) is an analytical model of the fuzzy PID controller.

3. AGA-based optimal fuzzy pid controller design

The design of a fuzzy PID controller can be treated as a multi-objective optimisation problem. The tuning of the fuzzy PID parameters is designed to achieve the best compromise between the rapidity, stability and accuracy of the system control. It is difficult to optimise all aspects of the overall performance at the same time through the general adjustment of fuzzy PID parameters. To address this problem, the current paper describes the application of GA to the fine tuning of the parameters for fuzzy PID controllers.

We propose an improved multi-objective optimisation method for parameter tuning of a fuzzy PID controller based on an adaptive genetic algorithm, which consists of the following five steps:

— **Step 1: Representation of the parameters**
In most applications of genetic algorithms to optimisation problems, the real coding technique is used to represent a solution to a given problem. In a real coding

https://doi.org/10.1017/S096012951300073X Published online by Cambridge University Press

implementation, each chromosome is encoded as a vector of real numbers of the same length as the solution vector. One of the key issues for the proposed AGA-based method is how to encode the parameters $x_i, y_j, K_p^{ij}, K_I^{ij}, K_D^{ij}$, for, $1 \leqslant i \leqslant n$,$1 \leqslant j \leqslant m$. The output trajectory of a sign-symmetry system is symmetrical to the original when the initial conditions and inputs are changed in sign. In many cases, like the AMB controller discussed in this paper, the system has a non-linear controller that is also sign-symmetric. We assume that the input variables $e(t)$ and $e(t)$ are divided into five fuzzy sets named:

- Negative Big (NB);
- Negative Small (NS);
- Zero (ZO);
- Positive Small (PS);
- Positive Big (PB).

The five fuzzy sets employ 50% overlapped triangular membership functions on the universe of discourse. Thus the parameters of the input variables can he simplified to the following four:

- the apex position $x4$ of PS;
- the apex position $x5$ of PB for $e(t)$;
- the apex position $y4$ of PM;
- the apex position $y5$ of PB for $e(t)$.

The PID expressions for the fuzzy control rule consequences each have three moduli and sign-symmetry. Therefore, when the membership functions of the input variables are symmetrical about 0, there are only 15 independent rules amongst the 25 fuzzy control rules described in (1). This means that there are only 49 parameters in the individual coding when implementing an AGA.

With the real coding implementation, the k chromosome of the l generation can be represented by

$$P_k^l = \left[x_{k4}^l, x_{k5}^l, y_{k4}^l, y_{k5}^l, K_{kP}^{ij^l}, K_{kI}^{ij^l}, K_{kD}^{ij^l}\right] = \left[p_{k1}^l, p_{k2}^l, \ldots, p_{k49}^l\right]. \tag{6}$$

Each chromosome p_k^l corresponds to 49 tuned parameters of the fuzzy PID controller.

— **Step 2: Design of the fitness function**

To evaluate the controller performance and get the required transient dynamic, the fitness function includes not only the four main transient performance indices (overshoot, rise time, settling time and cumulative error), but also a quadratic term in the control input to avoid the control energy becoming too big. The fitness function we designed is

$$J = 1 \Big/ \int_0^\infty [\omega_1 t e^2(t) + \omega_2 u^2(t)]dt + \omega_3 t_r + \omega_4 \sigma + \omega_5 t_s \tag{7}$$

where:

- $e(t)$ is the system error;
- $u(t)$ is the controller input;

https://doi.org/10.1017/S096012951300073X Published online by Cambridge University Press

- t_r is the rise time;
- σ is the maximal overshoot;
- t_s is the settling time with a 5% error band; and
- $\omega_1, \omega_2, \omega_3, \omega_4, \omega_5$ are weighting coefficients.

For a practical fuzzy PID design, we would adjust all the weighting coefficients in the fitness function according to the specific requirements for the system's rapidity, accuracy, stability, and so on. For example, if we require a system with a small overshoot value, we would increase ω_4 appropriately, but if we require a system with a fast dynamic response, we would increase ω_3. For this paper, we chose the weighting coefficients $\omega_i = 02$ for $i = 1, 2, \ldots, 5$ to cover all the performance indices completely.

— **Step 3: Selection**

In the proportional selection procedure, the selection probability of a chromosome is proportional to its fitness. However, this simple scheme has some undesired properties. To maintain a reasonable difference between the relative fitness ratings of the chromosomes and to prevent too rapid a takeover by some super chromosomes, we used an exponential ranking fitness assignment for the fitness calculations of the reproduction operator, because of its simplicity and robustness (Zhiming *et al.* 2003; Haiming and Yen 2003). The idea is straightforward: sort the population from best to worst and assign the selection probability of each chromosome according to its ranking rather than its raw fitness value. For the current paper, we chose normalised geometric selection, which is a ranking selection function based on a normalised geometric distribution.

— **Step 4: Crossover**

We used a single-point method for the crossover. Denoting two randomly selected chromosomes in the l generation by

$$P_k^l = [p_{k1}^l, p_{k2}^l, \ldots, p_{k49}^l]$$
$$P_q^l = [p_{q1}^l, p_{q2}^l, \ldots, p_{q49}^l],$$

the genetic values at the crossover point of these two chromosomes are p_{kj}^l and p_{qj}^l, respectively. Two new chromosomes are created after the crossover operation. The genetic values before and after the crossover point remain the same, while the genetic value of the crossover point is

$$\begin{aligned} p_{kj}^{l'} &= r_c p_{kj}^l + (1 - r_c) p_{qj}^l \\ p_{qj}^{l'} &= r_c p_{qj}^l + (1 - r_c) p_{kj}^l \end{aligned} \tag{8}$$

where r_c is a randomly generated constant between 0 and 1. For the current paper, we used the adaptive method, which takes the diversity of the population as the controlled variable, and we also adjusted the individual crossover rate based on the fitness value itself. The adaptive crossover rate for an individual is defined by

$$p_c = \begin{cases} \dfrac{k_c}{(f_{max} - f_{avg})/f_{avg}} + p_{c1} e^{\frac{c}{\tau_c}(f_c - f_{avg})} & f_c \geqslant f_{avg} \\[2ex] \dfrac{k_c}{(f_{max} - f_{avg})/f_{avg}} + p_{c1} & f_c < f_{avg} \end{cases} \tag{9}$$

https://doi.org/10.1017/S096012951300073X Published online by Cambridge University Press

where:

- f_{max} is the maximal fitness value of the present population;
- f_{avg} is the average fitness value of the present population;
- f_c is the larger fitness value of the two intersecting individuals;
- k_c, p_{c1} and p_{c2} are the crossover coefficients, with p_{c1} and p_{c2} having constant values between 0 and 1 with $p_{c1} > p_{c2}$;
- c is the crossover amplitude coefficient;
- and

$$\tau_c = \frac{f_{max} - f_{avg}}{\lambda_n(p_{c1}/p_{c2})}. \tag{10}$$

— **Step 5: Mutation**
We used a non-uniform mutation method. We set the mutated individual to be

$$P_k^l = [p_{k1}^l, p_{k2}^l, \ldots, p_{k49}^l]$$

after the mutation operation. The genetic value of an individual that is not mutated remains the same, while the gene $p_{kj}^{l'}$ for a mutated one is

$$p_{kj}^{l'} = \begin{cases} p_{kj}^l + \delta\left(l, p_{jmax} - p_{kj}^l\right) & r_m \geqslant 0.5 \\ p_{kj}^l - \delta\left(l, p_{kj}^l - p_{jmin}\right) & r_c < 0.5 \end{cases} \tag{11}$$

where r_m is a random number between 0 and 1, and $\delta(l, y)$ represents a random number within the range $[0, y]$, which varies with each generation evaluation. The expression for $\delta(l, y)$ is

$$\delta(l, y) = y(1 - r^{(1-\frac{l}{G})^b}) \tag{12}$$

where:

- r is a random number between 0 and 1;
- l is the current evolution generation;
- G is the set maximum evolution generation;
- b is a coefficient determining the dependency of the stochastic disturbance on the evolution generation l, which is generally determined by experience – for the current paper, we set $b = 2$.

For the current paper, we used the adaptive method, which takes the diversity of the population as the controlled variable, and we also adjusted the individual mutation rate based on the fitness value itself. The adaptive mutation rate for an individual is defined to be

$$p_m = \begin{cases} \dfrac{k_m}{(f_{max} - f_{avg})/f_{avg}} + p_{m1} e^{\frac{m}{\tau_m}(f_c - f_a vg)} & f_m \geqslant f_{avg} \\ \dfrac{k_m}{(f_{max} - f_{avg})/f_{avg}} + p_{c1} & f_m < f_{avg} \end{cases} \tag{13}$$

where:

- f_m is the fitness value of the individual undergoing the mutation operation;

https://doi.org/10.1017/S096012951300073X Published online by Cambridge University Press

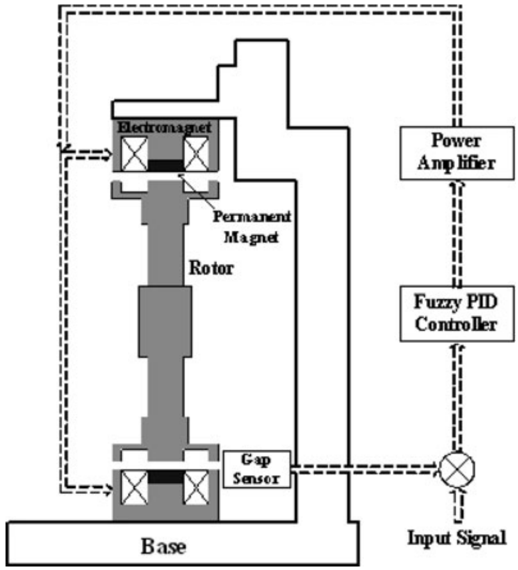

Fig. 2. Schematic of the controlled AMB system

- k_m, p_{m1} and p_{m2} are the mutation coefficients, with p_{m1} and p_{m2} having constant values between 0 and 1 with $p_{m1} > p_{m2}$;
- m is the mutation amplitude coefficient;
- and

$$\tau_m = \frac{f_{max} - f_{avg}}{\lambda_n(p_{m1}/p_{m2})}. \tag{14}$$

4. Analysis of the AMB system dynamic model

Figure 2 shows a schematic of the controlled AMB system. It consists of a levitated object (rotor) and a pair of opposing E-shaped controlled PM electromagnets with a coil winding. An attraction force acts between each pair of hybrid magnets and the extremities of the rotor. The attractive force each electromagnet exerts on the levitated object is proportional to the square of the current in each coil and is inversely dependent on the square of the gap. The entire system has only one degree of freedom for one axis, namely the axial position. Assuming a minimum distance for the length of the axis, the two attraction forces restrict radial motions of the axis in a stable way. The rotor position in the axial direction is controlled by a closed loop control system, which is composed of a non-contact type gap sensor, a Fuzzy PID controller and an electromagnetic actuator (power amplifier). This control is necessary since it is impossible to reach equilibrium using permanent magnets alone.

To model the AMB system, we assume a few simplifications:

(a) The rotor maintains symmetry around the rotating axis.
(b) Deviations around the normal operating point are small.

https://doi.org/10.1017/S096012951300073X Published online by Cambridge University Press

(c) The magnetic axial attraction force and the electromagnetic force are linearised around the operation point.

We assume: the mass of the suspended rotor is m; the hybrid magnets produce two attractive forces F_1 and F_2; and the applied voltage E from the power amplifier to the coil generates a current i, which is necessary only when the system is subjected to an external disturbance w. The equations governing the dynamics of the system are then

$$F_1(y,i) + F_2(y,i) - mg + w = m\frac{d^2y}{dt^2} \tag{15}$$

$$E = R_i + N\frac{d}{dt}(\phi_1(y,i) + \phi_2(y,i)) \tag{16}$$

where:

— y is the distance from the gap sensor to the bottom of the rotor;
— R is the resistance of the coil;
— N is the number of turns of the coil; and
— ϕ_1 and ϕ_2 are the flux in the top and bottom air gaps, respectively.

With a small disturbance, the above equation becomes

$$\Delta E = R\Delta t + N\frac{d}{dt}(\phi_1(y,i) + \phi_2(y,i)) \tag{17}$$

$$= R\Delta t + N\left(\frac{\partial(\triangle\phi_1 + \triangle\phi_2)}{\partial\Delta y}\frac{d\Delta y}{dt} + \right). \tag{18}$$

If the weight of the rotor is equal to the sum of these two attractive forces, the rotor will rotate with a specific gap. According to (14), the disturbance equation for a specific gap is calculated as follows:

$$\Delta F_1(\Delta y,\Delta t) + \Delta F_2(\Delta y,\Delta t) + w = m\frac{d^2\Delta y}{dt^2} \tag{19}$$

$$\Delta F_1(\Delta y,\Delta t) = \frac{\partial\Delta F_1}{\partial\Delta y}\Delta y + \frac{\partial\Delta F_1}{\partial\Delta t}\Delta t \tag{20}$$

$$\Delta F_2(\Delta y,\Delta t) = \frac{\partial\Delta F_2}{\partial\Delta y}\Delta y + \frac{\partial\Delta F_2}{\partial\Delta t}\Delta t. \tag{21}$$

We define

$$\phi = \phi_1 + \phi_2$$
$$F = F_1 + F_2.$$

The system is linearised at the operation point ($y = y_o, i = 0$) and is described as follows:

$$\frac{d^2\Delta y}{d\Delta y^2} = \frac{1}{m}\frac{\partial\triangle F}{\triangle y}\bigg|_{(y_0,0)}\Delta y + \frac{1}{m}\frac{d\Delta y}{dt}\Delta t + \frac{1}{m}w \tag{22}$$

$$\frac{d\Delta t}{dt} = -\frac{R}{L}\Delta t - \frac{N}{L}\frac{d\Delta\phi}{dy}\bigg|_{(y_0,0)}\frac{d\Delta y}{dt} + \frac{1}{L}\Delta E. \tag{23}$$

https://doi.org/10.1017/S096012951300073X Published online by Cambridge University Press

Table 1. *Centre and width values of the optimised membership function*

	$e(t)$		$\dot{e}(t)$	
	Centre	Width	Centre	Width
NB	−2.947	1.797	−149.600	217.198
NS	−1.203	2.947	−82.802	149.600
ZO	0	2.406	0	165.604
PS	1.203	2.947	82.802	149.600
PB	2.947	1.797	149.600	217.198

Then

$$\frac{d}{dt}\begin{bmatrix}\Delta y\\ \Delta y\\ \Delta i\end{bmatrix}=\begin{bmatrix}0 & 1 & 0\\ a_{21} & 0 & a_{23}\\ 0 & a_{32} & a_{33}\end{bmatrix}\begin{bmatrix}\Delta y\\ \Delta y\\ \Delta i\end{bmatrix}+\begin{bmatrix}0\\ 0\\ b\end{bmatrix}E+\begin{bmatrix}0\\ d\\ 0\end{bmatrix}w \tag{24}$$

where

$$a_{21}=\frac{1}{m}\frac{\partial \Delta F}{\partial y} \tag{25}$$

$$a_{23}=\frac{1}{m}\frac{\partial \Delta F}{\partial i} \tag{26}$$

$$a_{32}=-\frac{N}{L}\frac{\partial \Delta \phi}{\partial y} \tag{27}$$

$$a_{33}=-\frac{R}{L}b=\frac{1}{L}b=\frac{1}{m}L=N\frac{\partial \Delta \phi}{\partial \Delta y}. \tag{28}$$

The partial derivatives are calculated from the experimental characteristics at the normal equilibrium operating point. It can be seen from the characteristic roots that the system is unstable and controlling the AMB system is not an easy task. This system has to be stabilised by a controller with appropriate parameter tuning. In the following section, we will show that the fuzzy PID controller design drives the AMB system to an equilibrium position.

5. Simulation results and discussion

The AMB system shown in Figure 2 was used to demonstrate the feasibility of the proposed approach to dynamic systems. The fuzzy PID controller is designed using the proposed AGA. After 20 generations of the genetic operation, the resulting 49 optimal parameters describing the triangular membership functions and the PID gains of the fuzzy control rules are shown in Tables I and II, respectively.

The step responses of the rotor position from the gap sensor in the AMB system using the optimised fuzzy PID controller and the optimised conventional PID controller are shown in Figure 3. The figure shows that the fuzzy PID controller has achieved a remarkable reduction in the overshoot and settling time compared with the optimised conventional PID controller. The fuzzy PID controller also achieved good performance

https://doi.org/10.1017/S096012951300073X Published online by Cambridge University Press

Table 2. *The optimised PID gains for the fuzzy control rules*

K_P^{ij}		$e(t)$ NB	NS	ZO	PS	PB
$\dot{e}(t)$	NB	3.5497	3.6288	3.5979	4.2416	4.6291
	NS	3.6288	4.2586	4.5053	4.8485	4.0120
	ZO	3.5979	4.5053	4.1256	4.7111	3.2858
	PS	4.2416	4.8485	4.7111	3.3555	4.3927
	PB	4.6291	4.0120	3.2858	4.3927	4.5345
K_I^{ij}		$e(t)$ NB	NS	ZO	PS	PB
$\dot{e}(t)$	NB	1.7125	2.2040	1.5574	1.7037	2.5856
	NS	2.2040	1.3777	2.6298	2.1352	2.7379
	ZO	1.5574	2.6298	2.3093	2.4574	1.3506
	PS	1.7037	2.1352	2.4574	1.4898	2.1103
	PB	2.5856	2.7379	1.3506	2.1103	2.4721
K_D^{ij}		$e(t)$ NB	NS	ZO	PS	PB
$\dot{e}(t)$	NB	0.0396	0.0249	0.0129	0.0139	0.0396
	NS	0.0249	0.0318	0.0720	0.0992	0.0551
	ZO	0.0129	0.0720	0.0834	0.0110	0.0780
	PS	0.0139	0.0992	0.0110	0.0310	0.0196
	PB	0.0396	0.0551	0.0780	0.0196	0.0573

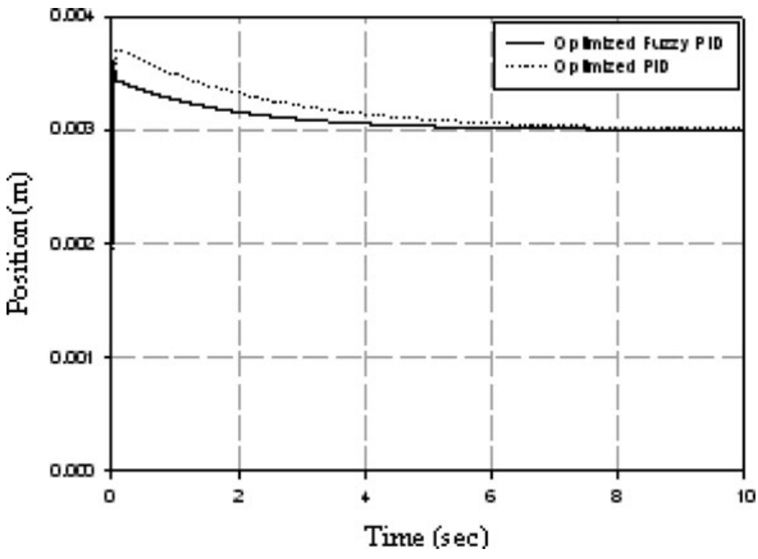

Fig. 3. The step responses of the rotor position from the gap sensor in the AMB system using the optimised fuzzy PID controller and the optimised conventional PID controller

for both transient and steady state periods. Figure 4 shows the converging patterns for the PID parameters. Moreover, the PID gains are adaptive and the fuzzy PID controller has greater flexibility and capability than conventional ones.

The variation of the best and mean fitness values given by the proposed AGA are plotted in Figure 5. Careful analysis of Figure 5 reveals that the best solution given by the proposed AGA in each population is being propagated to each subsequent generation

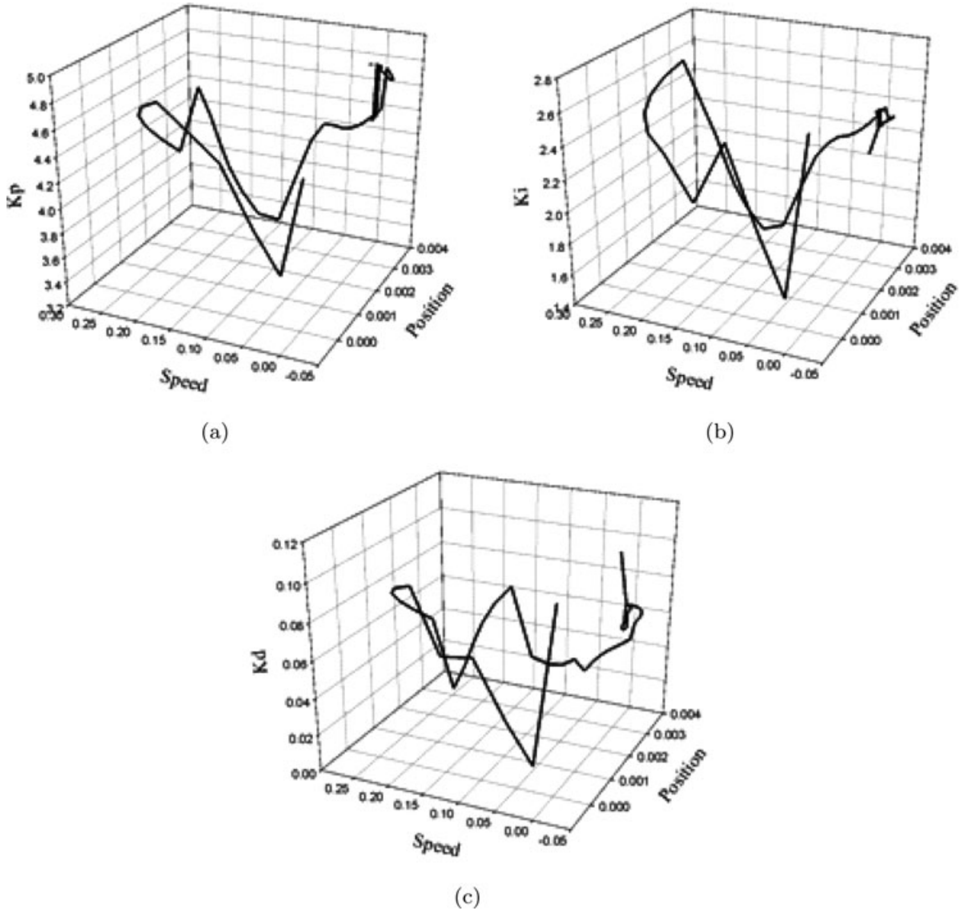

Fig. 4. Converging patterns for the PID parameters (a) K_p (b) K_i (c) K_d

and the best fitness is increasing with time. The lower mean fitness value of the proposed AGA indicates that the population has remained scattered in the solution space and has not become stuck at any local optimum. The optimisation efficiency is greatly enhanced by using AGA.

6. Conclusions

This paper has proposed an improved adaptive genetic algorithm for the multi-objective optimisation design of a fuzzy PID controller and applied it to the control of an AMB system. The proposed algorithm has better convergence speed and better stability in the global optimum result. Another benefit of the proposed method is the way it defines the fitness function based on the concept of multi-objective optimisation. This method allows the systematic design of all major parameters of a fuzzy PID controller, which enhances the flexibility and capability of the PID controller. Since the PID gains generated by the proposed approach are expressed in the form of fuzzy rules, they are more adaptive than

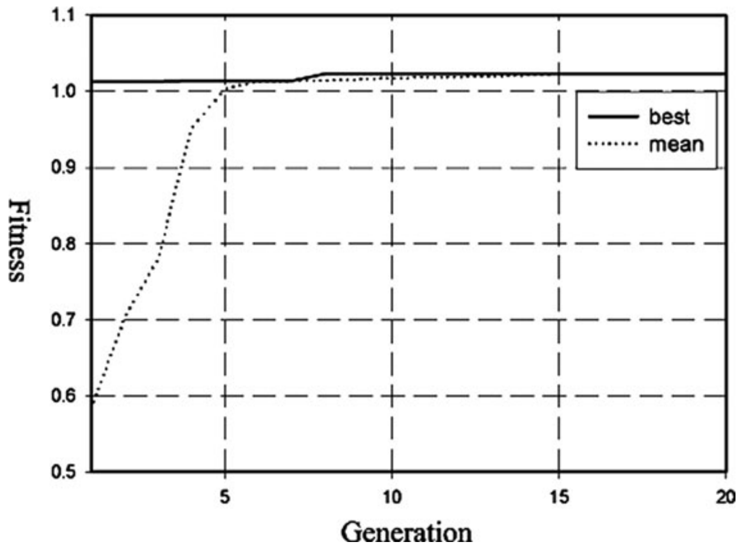

Fig. 5. The best and mean fitness values at each generation during the optimisation process

a PID controller with fixed gains. The simulation results for this AMB system show that a fuzzy PID controller designed using the proposed AGA has good performance.

References

Bennett, S. (1987) Development of the PID Controller. *IEEE Control Systems Magazine* **13** 58–65.

Chambers, L. (2001) *The Practical Handbook of Genetic Algorithms: Applications*, Chapman and Hall/CRC.

Chen, G. (1996) Conventional and Fuzzy PID Controller: An Overview. *International Journal of Intelligent Control Systems* **1** 235–246.

Chen, S. L. (2011) Nonlinear Smooth Feedback Control of a Three-Pole Active Magnetic Bearing System. *IEEE Transactions on Control Systems Technology* **19** (3) 615–621.

Fan, Y. H., Chen, K. Y., Weng, D. L. and Lee, Y. T. (2008) Design of Adaptive Compensator of Force Imbalance for a Single Active Magnetic Bearings Suspended Rotor System. *Journal of Applied Physics* **103** (7) 935–937.

Haiming, L. and Yen, G. G. (2003) Rank-Density-Based Multiobjective Genetic Algorithm and Benchmark Test Function Study. *IEEE Transactions on Evolutionary Computation* **7** (4) 325–343.

Harinath, E. and Mann, G. K. I. (2008) Design and Tuning of Standard Additive Model Based Fuzzy PID Controllers for Multivariable Process Systems. *IEEE Transactions on Systems, Man, and Cybernetics, Part B: Cybernetics* **38** (3) 667–674.

Khoo, W. K. S., Kalita, K., Garvey, S. D., Hill-Cottingham, R. J., Rodger, D. and Eastham, J. F. (2010) Active Axial-Magnetomotive Force Parallel-Airgap Serial Flux Magnetic Bearings. *IEEE Transactions on Magnetics* **46** (7) 2596–2602.

Knospe, C. R. (2007) Active Magnetic Bearings for Machining Applications. *Control Engineering Practice* **15** (3) 307–313.

Lin, L., L, L., Jan, H. Y. and Shieh, N. C. (2003) GA-Based Multiobjective PID Control for a Linear Brushless DC Motor. *IEEE Transactions on Mechatronics* **8** (1) 56–65.

https://doi.org/10.1017/S096012951300073X Published online by Cambridge University Press

Michalewicz, Z. (1996) *Genetic Algorithms + Data Structures = Evolution Programs*, Springer–Verlag.
Mohan, B. M. and Sinha, A. (2008) Analytical Structures for Fuzzy PID Controllers? *IEEE Transactions on Fuzzy Systems* **16** (1) 52–60.
Na, M. G. (2001) Auto-Tuned PID Controller Using a Model Predictive Control Method for the Stream Generator Water Level. *IEEE Transactions on Nuclear Science* **48** (5) 1664–1671.
Polajzer, B., Stumberger, G., Ritonja, J. and Dolinar, D. (2008) Variations of Active Magnetic Bearings Linearized Model Parameters Analyzed by Finite Element Computation. *IEEE Transactions on Magnetics* **44** 1534–1537.
Srinivas, M. and Patnaik, L. M. (1994) Adaptive Probabilities of Crossover and Mutation in Genetic Algorithms. *IEEE Transactions on Systems, Man and Cybernetics* **24** (4) 656–667.
Xiu, Z. and Ren, G. (2004) Optimization Design of TS-PID Fuzzy Controllers Based on Genetic Algorithms. In: *Proceedings of the 5th World Congress on Intelligent Control and Automation, Hangzhou, China* 2476–2480.
Zhiming, L., Jiliu, Z. and Su, L. (2003) New Adaptive Genetic Algorithm Based on Ranking. *Proceedings of the International Conference on Machine Learning and Cybernetics* **3** 1841–1844.